EXPERIMENTAL STUDY OF THE DEFORMATION OF PRINTING BLANKETS BY MEANS OF AN OPTICAL ANALYSIS

M.Sc. Mihael Gajičić [1], Prof. Dr. Karl Schaschek [1]
[1] Hochschule der Medien, Print and Media Technology, Stuttgart, Germany

Abstract: *The aim of this experimental study was to determine displacement and elastic strain of separate layers of different compressible printing blankets due to a uniaxial static plane pressure (plane-plane) using custom optical analysis methods. Compressible blankets are viscoelastic laminated compound structures composed of outermost incompressible printing rubber surface, several various stretch resistant supporting fabrics, and at least one compressible layer comprising a foamed rubber that may consist of voids or micro spheres. Depending on their mechanical characteristics, there are substantial differences in how these individual layers deform due to indentation by the plate or the impression cylinder in nip. In order to investigate these deformations, special equipment was built and techniques developed that allow precise contactless measurement of micro displacements. Series of microscopic images of a cross-section of blanket samples during gradually increasing plane indentation are acquired and the profiles of average Y-values of acquired images were plotted. Displacements of layer joints were defined exactly by the custom mathematical function using means of a maximum gradient search and strains were calculated according to the obtained results. Five different compressible blankets were studied and the results indicated that, in percentage rate, the top rubber layer of some blankets got more deformed than the rest of the blanket. This finding leads to the conclusion that some top rubber layers are more resilient than rest of layers.*

Key words: printing blanket, deformations in nip, strain measurement, optical analysis

1. INTRODUCTION

Thanks to the modern mechanical engineering, offset printing today stands for a relative stable and predictable printing process in which the most important parameters of machines are firmly defined or easily adjustable. There is a variety of printing blankets in use but some important characteristics that could help printers achieving desired results are not clearly declared. Because of their non-uniformity and inhomogeneity, blankets can have different characteristics in print. In several studies, the blankets were observed as homogeneous material, and this paper shows analysis of individual layers of blankets.

1.1 Offset printing

Offset printing is an indirect printing technology in which the printing ink is transferred from an offset plate to the blanket and then to the printing substrate (DIN 16529, 1982). There are sheet-fed and web-fed offset printing techniques. The centerpiece of every offset printing machine consists of three coupled cylinders: plate cylinder, blanket cylinder and impression cylinder (Figure 1a). The blanket cylinder is covered with the printing blanket in order to transfer ink from the plate to the substrate due to indentation in nip (Figure 1b) and therefore has a direct influence on print quality.

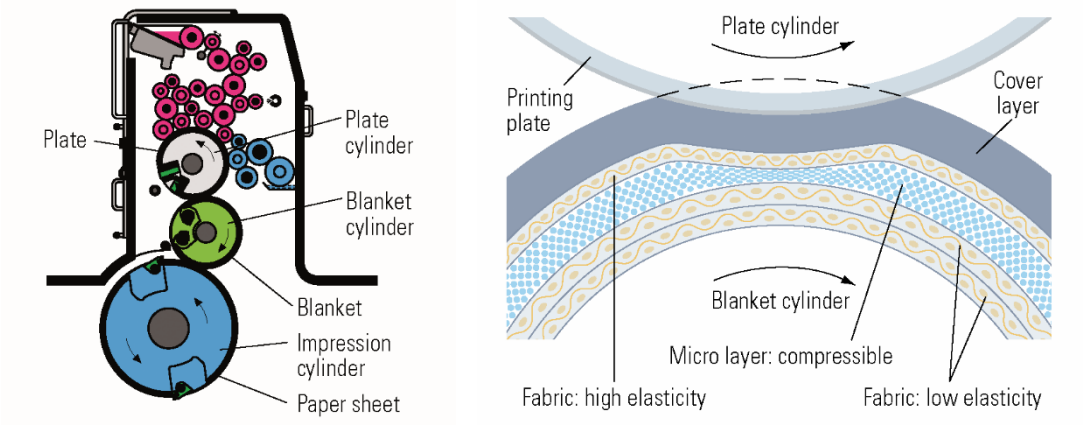

Figure 1: Cross-section of offset printing machine: a) offset printing unit (Kipphan,2001) b) blanket in nip (ContiTech)

1.2 Printing blankets

Incompressible and compressible blankets (Figure 2a) have to be distinguished and in this experimental study, several compressible blankets were investigated. Compressible blankets are compound laminated viscoelastic structures 1,65 to 1,95 mm thick (Walensky, 1993), composed of outermost incompressible rubber surface, multiple stretch resistant fabric plies and at least one compressible layer comprising a soft and resilient foamed rubber (Figure 2b). The latter one may consist of voids or micro spheres. Compressible blankets displace less rubber in nip than conventional ones, thus contributing to the attainment of true rolling or absence of tangential force and consequently less slippage (Riedl et al, 1989).

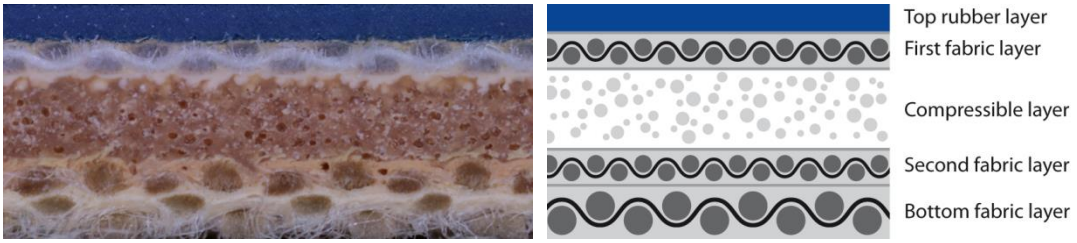

Figure 2: Structure of blanket: a) cross-section of compressible blanket b) layers of compressible blanket (One mostly used general model is displayed, variety of different blanket models are possible)

Depending on mechanical and viscoelastic characteristics of the individual layers, there are substantial differences in how these layers deform in nip due to indentation of neighbouring cylinders (Figure 3).

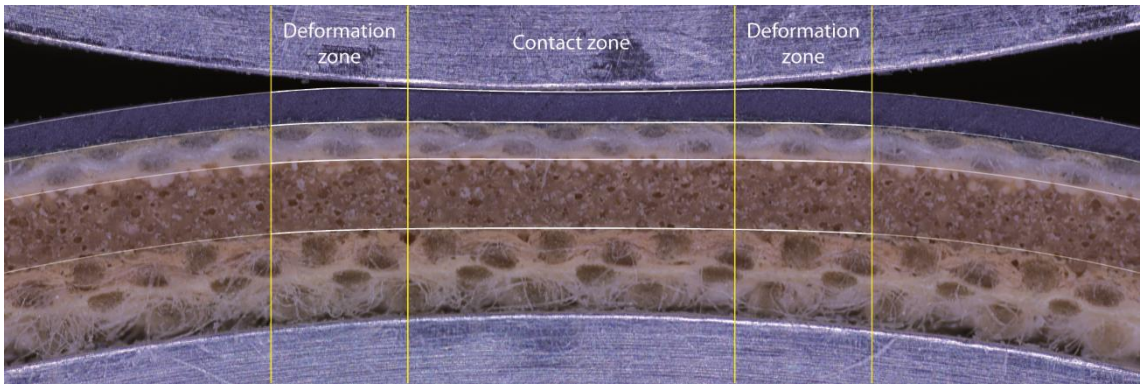

Figure 3: Cross-section of compressible printing blanket under indentation in simulated static nip (First two layers are relatively rigid and the radial displacement starts wide before and after the contact zone)

1.3 Viscoelasticity

Viscoelasticity is the property of material to exhibit simultaneously elastic and viscous characteristics. Their behavior may be represented by means of mechanical or rheological models composed of elastic and viscous elements (Hying, 2003). The mechanical behavior of an ideal elastic body obeys the Hooke-Law of elasticity E and is modeled with a linear elastic spring (Figure 4a) with a stress σ dependent and time t independent strain response ε (Figure 5a). The mechanical behavior of a viscous material is determined by the Newton-Law of viscosity η and is modeled with an ideal damping element (Figure 4b) that extends proportionally to the stress with a strain independent but time dependent response (Figure 5b). Maxwell viscoelastic model (Figure 4c) can be represented by an elastic spring and viscous damper connected in series, with a strain and time dependent response (Figure 5c). Kelvin–Voigt viscoelastic model (Figure 4d) consists of a Hookean elastic spring and a Newtonian damper that are connected in parallel, with a strain and time dependent response (Figure 5d). These two are the simplest viscoelastic models so that more realistic viscoelastic responses can be modelled using more elements (Kelly, 2016).

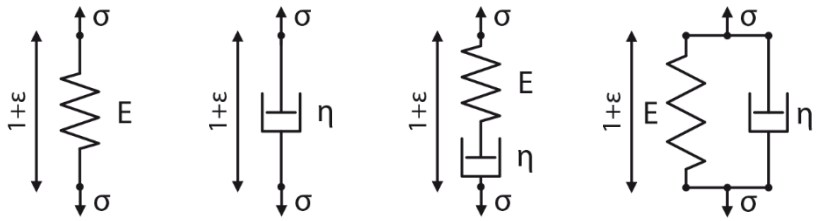

Figure 4: Mechanical element of elasticity and viscosity and models of viscoelasticity a) Hooke-Element b) Newton-Element c) Maxwell model d) Kelvin–Voigt model

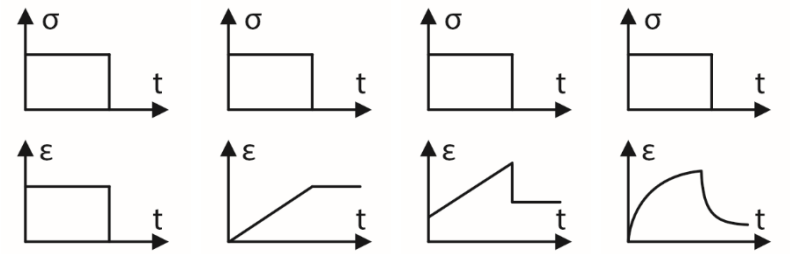

Figure5: Stress-strain responses of elastic and viscos element and viscoelastic models a) Hooke-element b) Newton-element c) Maxwell model d) Kelvin–Voigt model

1.4 Blanket model

Blankets are viscoelastic compounds and should be simulated with a couple in series and parallel connected viscoelastic models (Figure 6a). In this study, all experiments were static so the viscous component was neglected and blankets were modeled as ensemble of ideal springs in series (Figure 6b).

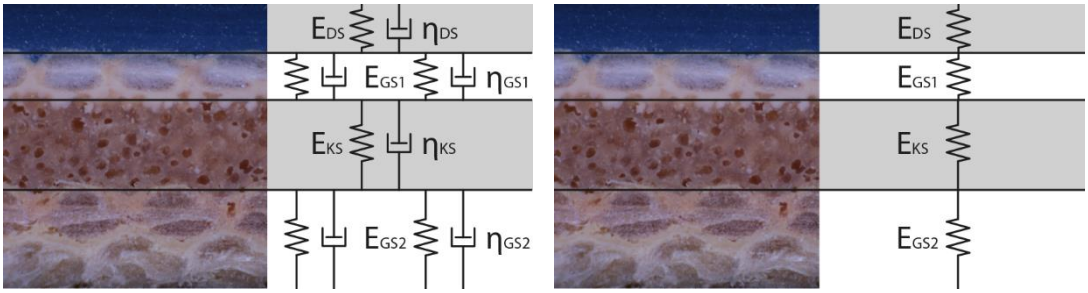

Figure 6: One-dimensional models of blanket: a) viscoelastic model b) simplified elastic foundation model (Blanket model in Figure 6b is only allowed if the system is considered as static and thus is examined)

For the springs in series, the stress applied to the ensemble gets equally applied to each spring, and the amount of strain is the sum of the strains of the individual springs. For parallel springs, the strain of the ensemble is their general strain and the stress of the ensemble is the sum of their stresses (Table 1).

Table 1: Stress and strain equations of springs in series and in parallel

	Springs in series	Springs in parallel
Strain	$\varepsilon = \varepsilon_1 + \varepsilon_2 + \varepsilon_3 + \varepsilon_N$	$\varepsilon = \varepsilon_1 = \varepsilon_2 = \varepsilon_3 = \varepsilon_N$
Stress	$\sigma = \sigma_1 = \sigma_2 = \sigma_3 = \sigma_N$	$\sigma = \sigma_1 + \sigma_2 + \sigma_3 + \sigma_N$

For the system of N linear elastic ideal springs in series, end-to-end, with elastic modulus of individual springs $E_1, E_2, E_3 \ldots E_N$ the equivalent elastic modulus E of an ensemble of springs can be calculated:

$$\frac{1}{E} = \sum_{i=1}^{N} \frac{1}{E_i} = \frac{1}{E_1} + \frac{1}{E_2} + \frac{1}{E_3} \ldots \frac{1}{E_N} \quad (1)$$

For the same ensemble of springs connected in parallel, side-by-side, the equivalent elastic modulus is:

$$E = \sum_{i=1}^{N} E_i = E_1 + E_2 + E_3 + \cdots + E_N \quad (2)$$

Based on Hooke's law $E = \sigma/\varepsilon$ and using relation (1), the elastic modulus of each layer of blanket can be calculated if the modulus of the blanket and strains of layers under indentation are known (Figure 7).

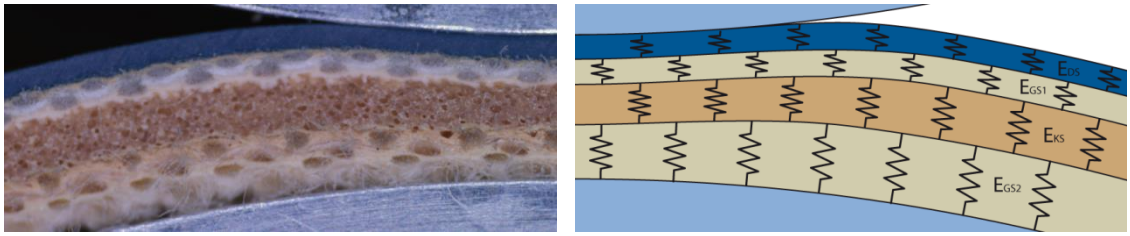

Figure 7: Printing blanket in nip: a) real blanket under indentation b) elastic foundation model of blanket (as a result of tangential resistance, the layers in the inlet and outlet zone are deformed without a kink)

The indentation and radial deformation of blanket consequently result in displacement of tangential direction, especially of incompressible layers (Figure 8), however, they are not analyzed in this study.

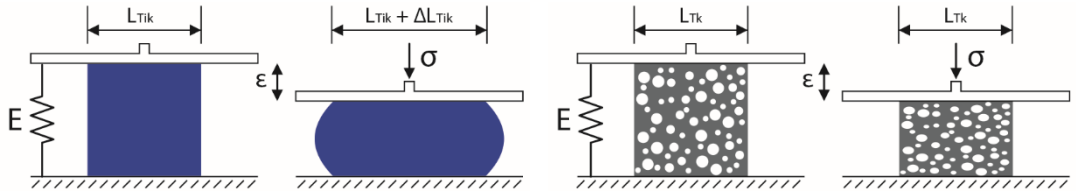

Figure 8: Horizontal displacements of two different materials under vertical pressure with consideration of friction a) ideal incompressible material with horizontal flow b) ideal compressible material without horizontal flow

2. METHODS

This study is focused on the use of special equipment and analysis techniques for the accurate and contactless measurement of displacement and the resulting micro strain and compression, specifically developed for this study. Even though they are in use in other technical sectors, these techniques were not used for printing blankets. Four main segments of this investigation are sample clipping and preparation, plane-plane and round-round indentation, acquisition of microscopic images of sample cross-sections and analysis of resulting strain and displacements.

2.1 Preparation of samples

For microscopic observation, multiple samples in size of 20 mm x 5 mm were cut. In microscopy, the depth of field is generally shallow, especially in devices without variable aperture and with large magnification. Therefore, a plane cross-section of observed sample is essential. In order to get the plane section of samples as smooth as possible, and to minimize squeeze, a sharp cutter was used. If not used, the sections would be always jagged and wavy, because of the horizontal material flow especially of very elastic and incompressible layers caused by vertical pressure of blade (Figure 8). Due to blankets inhomogeneous structures, there is unequal local stiffness and thus displacement and deformation of individual layers are not uniformly distributed over the surface. They strongly depend on the place of measurement or, if visually examined, on cross-section position and direction. Fabric layers are grid structures and their local resilience substantially affects displacement of other layers. Strength and thickness of warp threads are greater than of weft threads, and if cut along them and hit upon middle of one of these threads (Figure 9a), it appears fabric layer to be stiffer and other layers more resilient, however, it is contrariwise if cut between them (Figure 9c). The same happens if dissected across the blanket and hit upon middle of one of weft threads or between them.

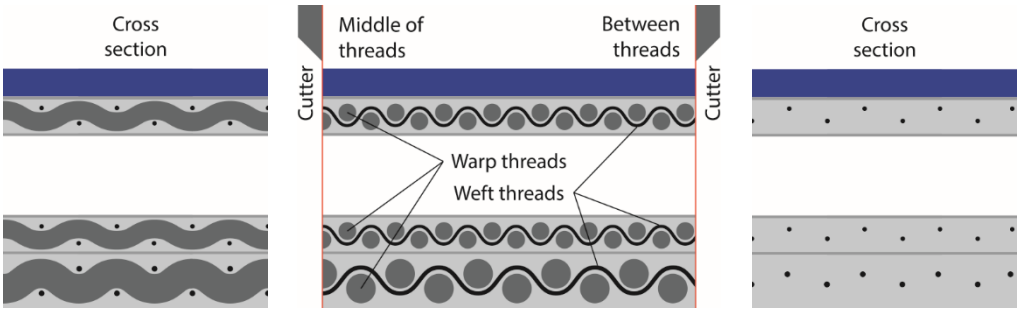

Figure 9: Model of blanket cross-section: a) cut upon middle of threads b) threads in blanket c) cut between threads (Because of the grid structure and inhomogeneity of layers, the best results were gained if blanket was cut diagonally)

It has become evident that most reliable results are gained by clipping the samples diagonally. Thus, elastic moduli of the warp and weft threads, as well as of their binding material, averaged over measured length. Thereby, the influence of distinctive inhomogeneity on the gained results is minimized.

2.2 Image acquisition

For the observation of deformations and image acquisition an optical stand microscope with a digital reflex camera and a precision cross table was additionally equipped. The device was automated with Arduino and driven by three stepper motors, one for each cross-table axis and one for a microscope focus adjustment. The resolution of cross-table was calculated to 0,625µm in both directions, so the sample could be very precisely led and positioned. The microscope was calibrated and with the maximal camera resolution of 6.000 x 4.000 pixels, whereas 1 pixel had a size of 0,459 µm so that with a single acquired image, an area of 2.754 µm x 1.836 µm could be taken. Magnification of the objective was 5x and multiplied with the 10x magnification of the ocular, it resulted in the total magnification up to 50x. In order to get high-resolution microscopic photos of the whole region of interest for every step of indentation, multiple images with defined overlap were acquired, and stitched with ImageJ plugin (Figure 10a). With every step of indentation, the cross-section of the sample becomes more uneven so the focus was readjusted in several distances in accordance with the relief of cross-section and the new series of photographs were taken. These multiple stitched photos were then stacked with ImageJ (Figure 10b). The result was the increase of depth of field and consequently supersized well-focused images (Figure 10c).

Figure 10: Acquisition and preparation of multiple microscopic images in order to get one supersized image a) stitching of ten images b) stacking of five stitched images c) one well-focused result image in high-resolution

The number of acquired single photos I_S could be calculated as a product of number of images along I_{Nx} and across I_{Ny} of the field of interest, indentation steps N_S and focus adjustment levels N_M:

$$I_S = I_{Nx}\, I_{Ny}\, N_S\, N_M \tag{2}$$

Total size in pixels of resulting image I_R along I_{Rx} and across I_{Ry} of the photographed sample can be calculated if the number of acquired images in both directions I_{Nx} and I_{Ny} as well as width I_{Sx} and height I_{Sy} of a single image is known and if overlap in both directions O_x and O_y are exactly defined:

$$I_R = I_{Rx}\, I_{Ry} = (I_{Nx}\, I_{Sx} - O_x\, I_{Nx} + O_x)(I_{Ny}\, I_{Sy} - O_y\, I_{Ny} + O_y) \tag{3}$$

The image acquisition process was fully automated and with this technique it was possible hundreds of images to make as well as to stitch and stack them in short time in order to prepare them for analysis.

2.3 Sample indentation

For this study, an indenter, based on a single-axis precision table, was constructed. The table was automated with Arduino, with one stepper motor driven and mounted on the cross table of microscope. Stepper motors usually have resolution of 200 steps per revolution but with an appropriate driver these full steps were split to 16 micro steps and overall resolution increased to 3.200 micro steps per revolution. The smallest indentation increment was defined as a quotient of thread pitch T_P of the precision table and the total number of steps S_R per revolution. For this device, the indenter resolution I_R was calculated to 0,625 µm, however, while unloaded, it was measured to 0,619 µm. This relative small difference could be probably ascribed to the imprecision of the thread pitch or less likely to the play of thread.

$$I_R = \frac{T_P}{S_R} = \frac{2000\ \mu m}{3200} = 0{,}625\ \mu m \tag{4}$$

Furthermore, a flexible fastening device was built and different indenters made. To ensure straight and to both indenters parallel displacements of individual joints of layers, which could be defined and tracked by the software in the further investigation step, plane indenters were required (Figure 11a). For a visual representation of displacements in static simulated nip, round indenters were used (Figure 11b).

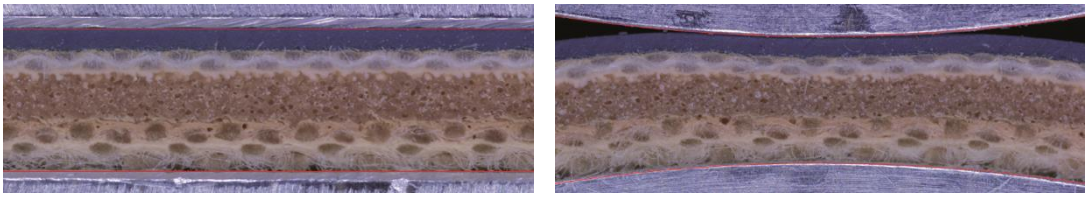

Figure 11: Sample indentations: a) plane indentation (plane-plane) and b) simulated nip (round-round) (Plane indentation provides reliable analysis of strains while all displacements are straight and parallel)

The top rubber layer, as the only incompressible layer, starts from some point of increasing indentation to well out and appears to be thicker but in this range of deformation measurement could it be neglected.

2.4 Analysis of deformations

To define the displacements of individual layers and to calculate their strain for every step of indentation the series of resulting photos were analyzed. They were loaded in ImageJ stack, and the profiles as average of 8-bit Y-values of every image with a customized macro were exported. The only manual step in the analysis was to determine approximately positions of layer joints of interest in the first image and so to define borders that should be tracked by the software. The exported values were loaded with custom Scilab macro and the maximal gradients in the manual defined areas of interest were found in the first image and then tracked successively in entire image series. For the starting points of the joints in every current image were the positions of the joints from the previous image used and so large displacements in relatively small indentation steps were traceable (Figure 13). The found joints (in Figure 12 as A, B and C marked) were as straight lines on the corresponding image displayed and so the analysis was visually proved. This study was focused in particularly on the strain of the top rubber layer S_{AB} and the rest of layers S_{BC} of investigated blanket S_{AC} so that the positions of these joints were of major interest. When the positions are exactly defined as P_A, P_B and P_C (Figure 12) their thickness T_{AB}, T_{BC} and T_{AC} as well as their strain in every indentation step i starting from the first image s could be calculated as follows:

$$S_{AB_i} = \frac{T_{AB_i}}{T_{AB_s}} - 1 = \frac{\left(P_{B_i} - P_{A_i}\right) - \left(P_{B_s} - P_{A_s}\right)}{P_{B_s} - P_{A_s}} \tag{5}$$

$$S_{BC_i} = \frac{T_{BC_i}}{T_{BC_s}} - 1 = \frac{\left(P_{C_i} - P_{B_i}\right) - \left(P_{C_s} - P_{B_s}\right)}{P_{C_s} - P_{B_s}} \tag{6}$$

$$S_{AC_i} = \frac{T_{AC_i}}{T_{AC_s}} - 1 = \frac{\left(P_{C_i} - P_{A_i}\right) - \left(P_{C_s} - P_{A_s}\right)}{P_{C_s} - P_{A_s}} \tag{7}$$

Gained values are calculated with (5,6,7) and shown in Table 2 as well as visually represented in Figure 13. Negative strain values mean that the layers were compressed and not stretched due to indentation.

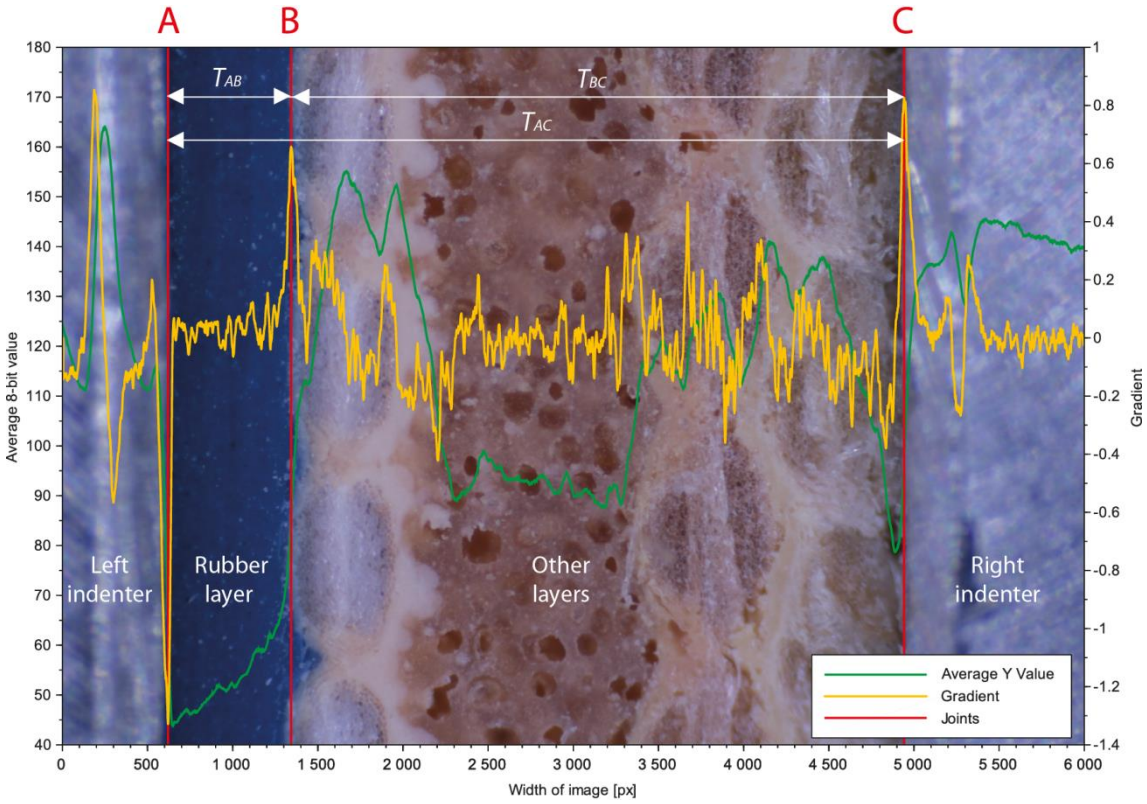

Figure 12: Defined layer joints of interest of analyzed printing blanket with average Y-values gradients and layer joints (Line A is the top side of the blanket and line C is the bottom side. Line B defines the distribution of total deformation)

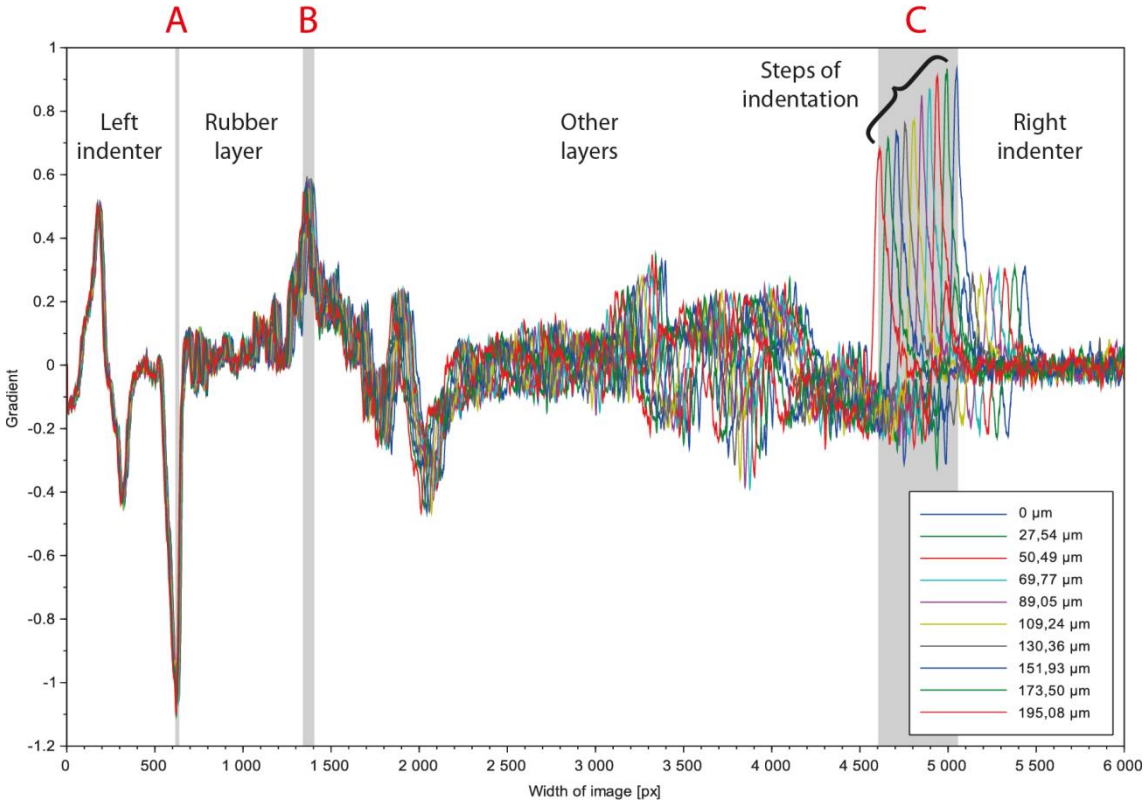

Figure 13: Gradient of average Y-values of image series of printing blanket under increasing plane indentation

As in Figure 13 shown, the right indenter (area C) had the largest displacement because all experiments were performed with them (right to left) and the left one was fixed. Left indenter (area A), though, had some displacement and that could be ascribed to the elasticity of testing device. Both of these displacements were tracked and strains considering measured positions calculated. Joint B defines how the overall deformation of blanket (AC) on the top rubber layer and the other layers is distributed (area B).

Table 2: Measured displacements and calculated strain for one sample

	Indentation [µm]	Position [px]			Thickness [µm]			Strain [%]		
		P_A	P_B	P_C	T_{AC}	T_{AB}	T_{BC}	S_{AC}	S_{AB}	S_{BC}
Image 1	0,00	627	1.400	5.048	2.029,24	354,81	1.674,43	0,00	0,00	0,00
Image 2	27,54	630	1.388	4.991	2.001,70	347,92	1.653,78	-1,36	-1,94	-1,23
Image 3	50,49	628	1.385	4.939	1.978,75	347,46	1.631,29	-2,49	-2,07	-2,58
Image 4	69,77	627	1.380	4.896	1.959,47	345,63	1.613,84	-3,44	-2,59	-3,62
Image 5	89,05	625	1.374	4.852	1.940,19	343,79	1.596,40	-4,39	-3,10	-4,66
Image 6	109,24	623	1.369	4.806	1.920,00	342,41	1.577,58	-5,38	-3,49	-5,78
Image 7	130,36	621	1.364	4.758	1.898,88	341,04	1.557,85	-6,42	-3,88	-6,96
Image 8	151,93	619	1.358	4.709	1.877,31	339,20	1.538,11	-7,49	-4,40	-8,14
Image 9	173,50	617	1.352	4.660	1.855,74	337,37	1.518,37	-8,55	-4,92	-9,32
Image 10	195,08	614	1.347	4.610	1.834,16	336,45	1.497,72	-9,61	-5,17	-10,55

The layers were characterized with a slope of regression line of measured curves in deformation area important for technical application and afterwards the gained values were used for layer comparison.

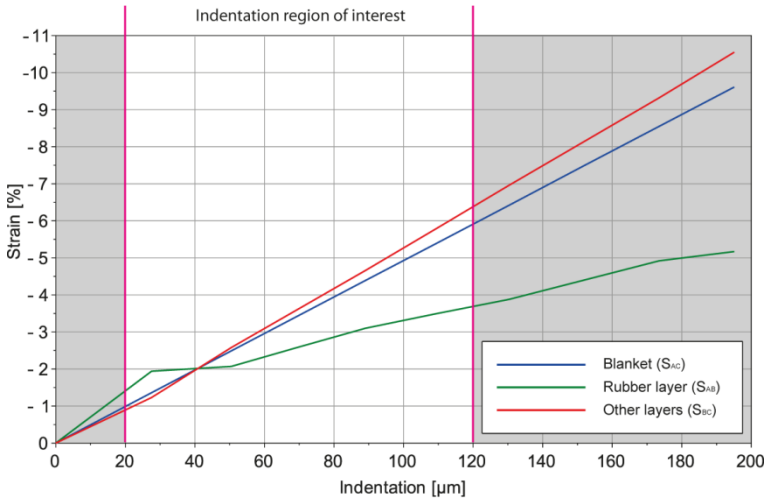

Figure 14: Deformation of individual layers of printing blanket
(Indentation region of 20 to 120 µm corresponds to the indentation in printing machine)

The analysis was very reliable when layers were straight, visually clearly separated and in different colors. Otherwise the process fails because the gradients of gained curves were not enough distinct. That was the main disadvantage of this automatic analysis technique. In some cases, there was significant improvement of layer distinction achieved by enhancing contrast of images or by splitting color channels.

3. RESULTS

In this research there were samples of five printing blankets with different structure as well as mechanical and geometrical characteristics investigated (Figure 15). The samples are adequately prepared according to the capital 2.1 and then the plain indentations performed as in capital 2.3 depicted. Microscopic images were acquired as in capital 2.2 described, and image series were analyzed as in 2.4 explained.

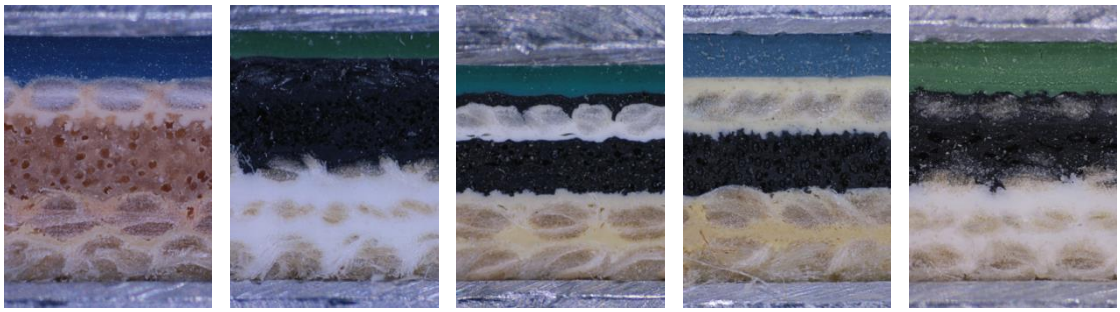

Figure 15: Five investigated compressible printing blankets
a) Blanket 1 b) Blanket 2 c) Blanket 3 d) Blanket 4 e) Blanket 5

The thickness of the entire non-deformed and unstrained blankets and of their separate layers of interest are precisely defined and used in the further strain calculation. All investigated blankets and their individual layers had significantly different thicknesses (Table 3). Since all samples were measured and investigated tangentially unstrained, they appeared up to 5 percents thicker as manufacturer specified.

Table 3: Thickness of non-deformed and unstrained blankets and separate layers of interest

Thickness [µm]	Blanket 1	Blanket 2	Blanket 3	Blanket 4	Blanket 5
Blanket (AC)	2.001,62	2.028,24	1.759,27	1.993,36	1.927,91
Top layer (AB)	334,84	215,42	233,019	352,36	410,8
Other layers (BC)	1.666,78	1.812,82	1.526,25	1.641,00	1.517,11

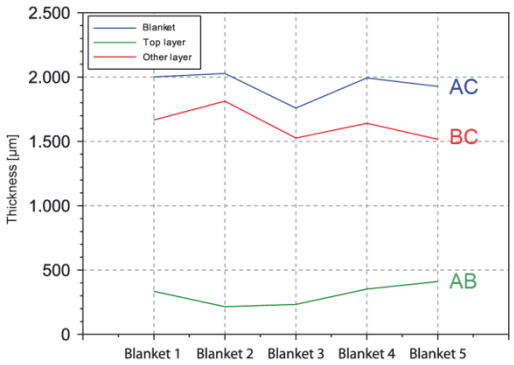

Figure 16: Thickness of investigated printing blankets and their individual layers of interest

The second investigated blanket was the thickest one but had the thinnest top layer. The third blanket was overall the thinnest and the fifth one had the thickest top rubber layer (Figure 16). In order to get the reliable results and to minimize the effect of blanket inhomogeneity, five separate samples of every blanket were investigated and the gained results were averaged and visually presented (Figure 17).

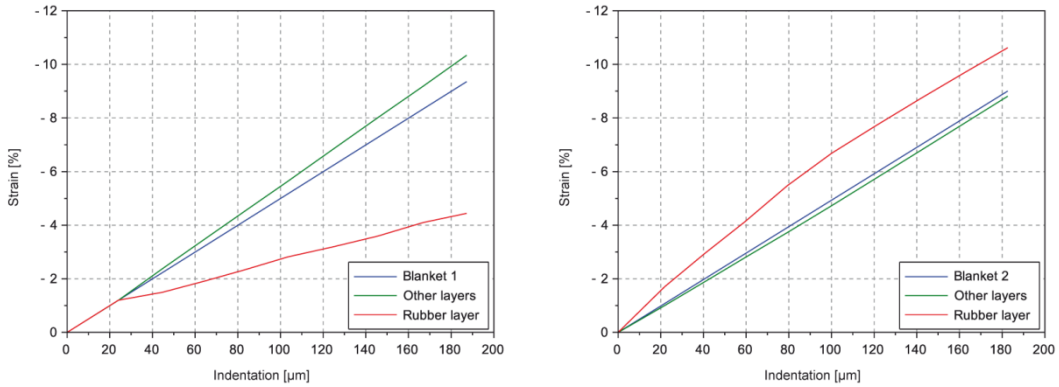

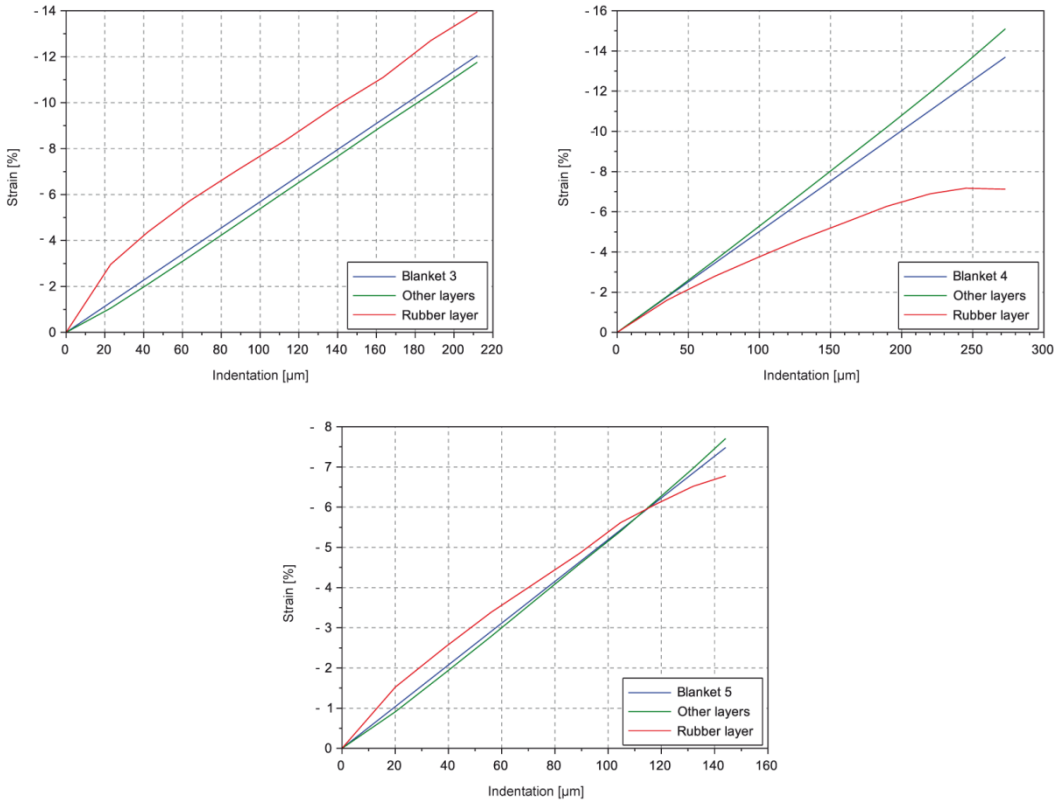

Figure 17: Results of displacement measurement and strain calculation of five studied blankets

As it can be seen in Figure 17, the top layer of the first investigated blanket was the least compressed under same indentation and the top layer of the third blanket the most. The rest of layers were deformed similarly to the whole blanket because they comprise the largest part of them. In order to compare the strain values and to make them relevant to the real condition in offset printing, the linear regressions of stress-strain curves were calculated in area from 20 to 120 µm (Engelmann et al., 1962) of indentation and their slopes were defined (Table 4). The slope of stress-strain curve correlates with the deformation and with the E modulus of the corresponding layer and provides information of its behavior in the nip.

Table 4: Slopes of regression lines of measured stress-strain curves of blankets and of separate layers of interest

	Blanket 1	**Blanket 2**	**Blanket 3**	**Blanket 4**	**Blanket 5**
Blanket (AC)	-0,0500	-0,0493	-0,0568	-0,0502	-0,0519
Top layer (AB)	-0,0205	-0,0613	-0,0582	-0,0321	-0,0465
Other layers (BC)	-0,0559	-0,0479	-0,0566	-0,0540	-0,0536

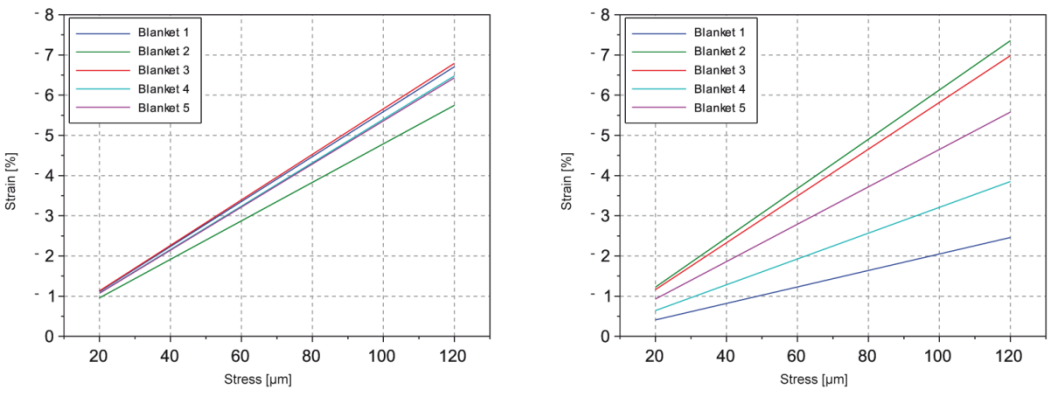

Figure 18: Calculated stress-strain curves a) other layers b) top rubber layers

In the area of deformation of interest, the top layer of the first blanket has the smallest slope of regression line, and the first layer of the second blanket, the largest one (Table 4). This indicates that the first layer of the first blanket gets less compressed and has larger elastic modulus than the rest of the blanket. On the other hand, at the second blanket, the difference between the modulus of the first layer and the rest of them is not as big as at the first blanket and the modulus of the first layer is smaller since it gets more deformed than of the rest layers of the blanket. The results show that the total deformation of different blankets is differently distributed in separate layers, depending on their elastic modulus. The largest strain difference was measured in top layers (Figure 18b) and the other layers have relatively similar strain response to applied stress (Figure 18a).

4. CONCLUSIONS

This study was performed by assumption that separate layers of printing blankets might be differently deformed due to the same indentation by the plate or the impression cylinder in the nip depending on their mechanical and viscoelastic characteristics. For this purpose, the special equipment was constructed and automated, that allows very precise indentation of specimens and microscopic image acquisition. Furthermore, the analysis technique for accurate measurement of micro displacements and calculation of resulting strain was developed. The research has shown that the micro displacements of under 0,5 µm could be searched contactless and successfully tracked in series of microscopic images acquired during increasing indentation. Unequal thickness and radial compression of layers could consequently cause different tangential displacements, especially of incompressible layers and could have a great importance on the print quality and feeding characteristics of the blanket. The calculated slopes of regression lines of calculated strains and the measured thicknesses of top rubber layers could be used by estimation of tangential displacement of this layer in and around the nip. In further work, the tangential displacements will be investigated and visually presented, especially of the top rubber.

5. ACKNOWLEDGMENTS

This work is supported by the Hochschule der Medien in Stuttgart and financed by ContiTech Elastomer-Beschichtungen GmbH, Northeim, Felix Böttcher GmbH & Co. KG, Köln, Druckzentrum Rhein Main GmbH, Rüsselsheim am Main and Deutsche Forschungsgemeinschaft.

6. REFERENCES

[1] DIN 16529: Drucktechnik; Begriffe für den Flachdruck (November, 1982)
[2] Engelmann, A., Schwend, K.: „Der Offsetdruck aus der Praxis für die Praxis“, Otto Blersch Verlag, Stuttgart, 1962
[3] Hying, K.: „Analyse der viskoelastischen Eigenschaften von Poly(tetrafluorethylen) im Bereich des β-Übergangs“, Doktordissertation, Aachen, 2003
[4] Kelly, P.A.: “Lectures in Solid Mechanics Part I: Rheological Models”, URL http://homepages.engineering.auckland.ac.nz/~pkel015/SolidMechanicsBooks/Part_I/ (last request: 2016-09-21).
[5] Kipphan H.: „Handbook of Print Media”, Springer Verlag, New York, 2001
[6] Riedl, R, Neumann, D, Teubner, J.: „Technologie des Offsetdrucks“, Fachbuchverlag, Leipzig, 1989
[7] Walenski, W.: „Lexikon des Offsetdrucks“, Verlag Beruf+Schule, Itzehoe, 1993